Journal of Mathematical Physics

Stimulated Raman adiabatic passage-like protocols for amplitude transfer generalize to many bipartite graphs

Cite as: J. Math. Phys. **61**, 072201 (2020); https://doi.org/10.1063/1.5116655
Submitted: 26 June 2019 . Accepted: 17 June 2020 . Published Online: 06 July 2020

Koen Groenland, Carla Groenland, and Reinier Kramer

Journal of Mathematical Physics ARTICLE scitation.org/journal/jmp

Stimulated Raman adiabatic passage-like protocols for amplitude transfer generalize to many bipartite graphs

Cite as: J. Math. Phys. 61, 072201 (2020); doi: 10.1063/1.5116655
Submitted: 26 June 2019 • Accepted: 17 June 2020 •
Published Online: 6 July 2020

Koen Groenland,[1,a)] Carla Groenland,[2] and Reinier Kramer[3]

AFFILIATIONS

[1] QuSoft and CWI, Science Park 123, 1098 XG Amsterdam, The Netherlands and Institute of Physics, University of Amsterdam, Science Park 904, 1098 XH Amsterdam, The Netherlands
[2] Mathematical Institute, University of Oxford, Andrew Wiles Building, Radcliffe Observatory Quarter (550), Woodstock Road, Oxford OX2 6GG, United Kingdom
[3] Max-Planck-Institut für Mathematik, Vivatsgasse 7, 53111 Bonn, Germany

[a)] **Author to whom correspondence should be addressed:** koen.groenland@gmail.com

ABSTRACT

Adiabatic passage techniques, used to drive a system from one quantum state into another, find widespread applications in physics and chemistry. We focus on techniques to spatially transport a quantum amplitude over a strongly coupled system, such as STImulated Raman Adiabatic Passage (STIRAP) and Coherent Tunneling by Adiabatic Passage (CTAP). Previous results were shown to work on certain graphs, such as linear chains, square and triangular lattices, and branched chains. We prove that similar protocols work much more generally in a large class of (semi-)bipartite graphs. In particular, under random couplings, adiabatic transfer is possible on graphs that admit a perfect matching both when the sender is removed and when the receiver is removed. Many of the favorable stability properties of STIRAP/CTAP are inherited, and our results readily apply to transfer between multiple potential senders and receivers. We numerically test transfer between the leaves of a tree and find surprisingly accurate transfer, especially when straddling is used. Our results may find applications in short-distance communication between multiple quantum computers and open up a new question in graph theory about the spectral gap around the value 0.

I. INTRODUCTION

STImulated Raman Adiabatic Passage (STIRAP) is a technique typically applied in molecular and atomic physics, where it is used to transfer some internal state $|1\rangle$ to another state $|3\rangle$, by coupling both of these states to some intermediate state $|2\rangle$ by two tuned laser pulses.[1] An important feature is that state $|2\rangle$ is minimally populated, making the evolution largely insensitive to decoherence due to the intermediate state.[2] Such state transfer protocols have various applications, such as the preparation of useful quantum states, performing coherent quantum logic gates, or sending quantum information between spatially separated agents. STIRAP, in particular, is now widely adopted in fields where accurate control of quantum states is vital, such as high precision measurement,[3,4] studies of atoms and molecules,[5–9] and quantum information processing.[10–14]

The formalism has been generalized to work on systems where some (odd) N states are coupled in the form of a linear chain, allowing transfer between the endpoints of the chain.[15] A mathematically equivalent protocol can be used to spatially displace quantum amplitudes. In 2004, two independent works proposed state transfer of quantum particles over linear chains by tuning the hopping strengths instead of laser fields: Ref. 16 considered neutral atoms in optical lattices, while Ref. 17 addressed electron tunneling between quantum dots. The latter introduced the name Coherent Tunneling by Adiabatic Passage (CTAP), which we will also use to denote spatial transfer. Apart from

particle tunneling, the same model applies to ferromagnetic spins under XX interaction,[18] where a single spin excitation can be adiabatically transferred.

With the advent of quantum information processing, accurate control and high-fidelity qubit transport in increasingly large systems have become an important scientific challenge.[19,20] Whereas a large amount of work can be found on transfer over a linear chain of length 3 or N,[2,21] little is known about adiabatic transfer in more general systems. Notable exceptions are Refs. 22 and 23, which consider square and triangular grids, and Ref. 24, which addresses multiple parties dangling on a line, each of whom could send or receive the quantum state. Other works, such as Refs. 25 and 26, describe a variation where the chain splits into multiple paths or branched endpoints. These protocols are shown to work by a clever mapping back to the original protocol on the chain.

We present a completely different approach to find more general configurations that allow a similar transfer protocol by describing system's interactions in the language of graphs: the vertices represent basis states and edges represent interactions. We look at bipartite graphs, where the basis states can be separated into two sets V_1 and V_2 such that each state interacts only with states outside its own set. If the two sets differ in size by one, then amplitude transfer between states in the bigger set may be possible. We can guarantee successful transfer when certain graph properties are satisfied, as made precise in Theorem 3.

Interestingly, our approach naturally provides a means to transfer amplitude to one out of multiple potential receivers, generalizing Ref. 24. We find that the final receiver need not yet be known when starting the protocol, which could be an advantage in quantum information processing.

These results advance the fields of STIRAP and spatial transfer in two ways. First, they open the way to practical adiabatic passage in more general systems. Second, they shed light on possible perturbations in conventional STIRAP and their effect: we find that many perturbations, as long as they satisfy our assumptions, do not cause a qualitatively different effect on the state's evolution during the protocol.

Our treatment of bipartite graphs is reminiscent of the celebrated Morris-Shore (MS) transformation.[27] The transformation finds a unitary map A on the part V_1 and a unitary map B on part V_2 such that the system decomposes into a set of decoupled two-level systems and a set of uncoupled states. Similar to the setting of MS, we focus on the uncoupled states, which are called dark states. Our contribution is distinct from work related to MS transformations, due to the focus on adiabatic transfer techniques, in which the MS transformation would continuously change in time. Therefore, it is not immediately clear how MS could guarantee that our adiabatic state remains nondegenerate, and we choose to resort to other techniques.

Our work is also closely related to the field of perfect state transfer (PST), which addresses the same goal of transfer between two states $|a\rangle, |b\rangle$, in general graphs.[28] However, PST is concerned with *quenches* such that $|\langle b|e^{-iHt}|a\rangle| = 1$ for a time-independent Hamiltonian H. Therefore, PST is typically faster than adiabatic transfer, but it puts stringent constraints on the precise interaction strengths.

This paper is organized as follows: In Sec. II, we review the conventional STIRAP and CTAP protocol after which we present our main result on more general graphs in Sec. III. We then discuss the applicability in real-world systems in Sec. IV, and methods to obtain graphs that satisfy our assumptions in Sec. V. We numerically test the scaling of the adiabatic gap in various graphs, and the fidelity of our protocol, in Sec. VI and finish with a conclusion in Sec. VII.

II. CONVENTIONAL STIRAP

As its name implies, STIRAP makes essential use of the adiabatic theorem,[29] which states that if a system starts out in an eigenstate of the Hamiltonian whose eigenvalue is isolated, and the Hamiltonian changes slowly, the system remains in the same instantaneous eigenstate.

More precisely, suppose a Hamiltonian $H(s)$, depending smoothly on time $s \in [0, 1]$, has a smoothly varying basis of instantaneous eigenfunctions $|\phi_k(s)\rangle$ with eigenvalues $E_k(s)$. Let $\widetilde{H}(t) = H(t/T)$ be the time-rescaled Hamiltonian. Let $|\psi(t)\rangle = \sum_k c_k(t)|\phi(t/T)\rangle$ be the solution of the Schrödinger equation,

$$i\hbar \frac{d}{dt}\psi(t) = \widetilde{H}(t)\psi(t),$$

with $c_k(0) = \delta_{1k}$. If, for all s, $E_1(s) - E_k(s)$ is bounded from below by A_k, and all $\langle \phi_l(s)|\dot{\phi}_1(s)\rangle$ are bounded from above by Q, then[29]

$$|c_k(T) - \delta_{1k}| \propto \frac{Q}{A_k T}. \tag{1}$$

In other words, the difference between the instantaneous eigenstate of $\widetilde{H}(t)$ and the evolved state $|\psi(t)\rangle$ scales inversely with the time taken for the change and with the energy gap. This difference can be made arbitrarily small by choosing a sufficiently large T.

The conventional STIRAP protocol (Fig. 1) deals with a three-dimensional quantum system, consisting of eigenstates $\{|j\rangle\}_{j=1}^3$ of some background Hamiltonian. To transfer amplitude from $|1\rangle$ to $|3\rangle$, a sequence of two laser pulses is applied: the Stokes pulse coupling $|2\rangle \leftrightarrow |3\rangle$, and the pump pulse coupling $|1\rangle \leftrightarrow |2\rangle$. Throughout this work, we consider only the interaction picture and assume the rotating wave approximation to hold. The system's Hamiltonian then becomes

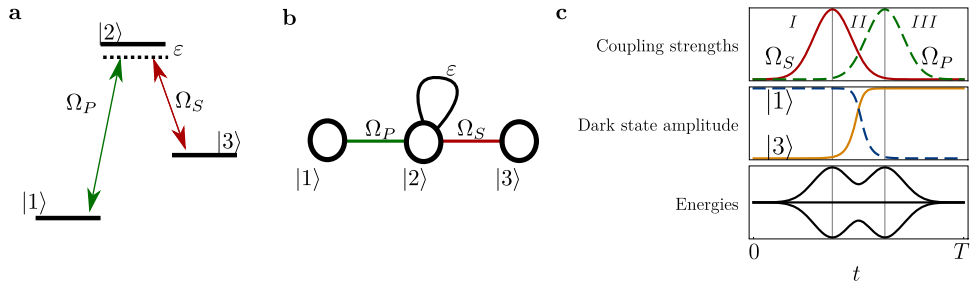

FIG. 1. The conventional STIRAP/CTAP protocol on a three-site Λ system. (a) The energy diagram of the three states, coupled by the Stokes (S) and Pump (P) lasers, also represented as a graph in (b). (c) Stacked plot showing the laser amplitudes, state amplitudes, and energies (eigenvalues λ) as a function of time in arbitrary units. Stages I and III involve turning the couplings on/off, whereas stage II constitutes the relevant adiabatic driving part, which transfers amplitude from state $|1\rangle$ to $|3\rangle$ as amplitudes Ω_S and Ω_P are slowly adjusted relative to each other. Reproduced with permission from Groenland, "Quantum protocols for few-qubit devices," ILLC Dissertation Series (University of Amsterdam, 2020).[43]

$$H = \begin{pmatrix} 0 & \Omega_P(t) & 0 \\ \Omega_P(t) & \varepsilon & \Omega_S(t) \\ 0 & \Omega_S(t) & 0 \end{pmatrix}. \tag{2}$$

Here, $\Omega_{S/P}$ denotes the Rabi frequency (amplitude) of the Stokes and pump lasers and ε absorbs the off-resonances, assuming that both are equal in size. One can check that one instantaneous eigenstate of H is the zero energy "dark state" $|z\rangle$ given by

$$|z(t)\rangle = \frac{1}{\mathcal{N}} \begin{pmatrix} \Omega_P^{-1}(t) \\ 0 \\ -\Omega_S^{-1}(t) \end{pmatrix},$$

where $\mathcal{N}$ denotes the normalization. The dark state $|z\rangle$ has precisely the property that it transitions from $|1\rangle$ to $|3\rangle$ as Ω_S is gradually diminished while Ω_P is increased. Note the counter-intuitive order of the pulses, as indicated in Fig. 1. A key property of STIRAP is that, under ideal circumstances, the excited state $|2\rangle$ is never populated during this process; hence, the protocol is independent of decoherence due to emission from this state. Thanks to this, and the inherent stability of adiabatic methods,[30] the protocol is relatively stable to experimental imperfections and is broadly adopted in practice.[2]

The setting where quantum particles can tunnel between three adjacent sites is mathematically equivalent to Eq. (2), where the parameters Ω now take the role of tunneling amplitudes. The same protocol can then be applied, leading to the transfer of the particle wavefunction, as is the case in CTAP.

III. GENERALIZING STIRAP

We observe that a key property of STIRAP and CTAP is the existence of a unique zero-energy eigenstate at all times and that this state is localizable by lowering couplings incident to a particular site. This leads us to our main question: which other physical configurations pertain *precisely* one zero eigenvector, even when uncoupling a certain site?

Note that the adiabatic theorem does not require the eigenvalue to be zero. Rather, it is an essential ingredient in our proofs, and it simplifies tracking the dynamical phase in experiments.

We capture the more general configurations in the language of (finite) *weighted graphs* $G = (V, E, w)$. Here, the collection of vertices $V = \{v_j\}_{j=1}^{\dim(\mathcal{V})}$ corresponds to a set of basis states $\{|v_j\rangle\}_{j=1}^{\dim(\mathcal{V})}$ of Hilbert space $\mathcal{V}$. Two vertices $v, u \in V$ are connected by an edge $uv \in E$ if and only if an interaction that couples states $|u\rangle$ and $|v\rangle$ can be applied. The weights $w : E \to \mathbb{C}$ assign a complex amplitude to each of the interactions. Weights evaluated on non-existent edges are zero: $w_{uv} = 0$ for all $uv \notin E$. In the context of CTAP, the vertices should be interpreted as sites for the particle, and the edges indicate possible tunneling of the particle. In the context of STIRAP, vertices are energy levels, and edges are possible couplings by laser fields.

The *adjacency matrix* A_G of a graph is then defined as the matrix of weights, with matrix elements $(A_G)_{uv} = w_{uv}$. We impose hermiticity through $w_{uv} = w_{vu}^*$. For computational simplicity, we take the adjacency matrix to be constant (we consider it as a background) and define the *control Hamiltonian* H_G for a given graph G by

$$H_G(t) = \sum_{u,v \in V} f_{uv}(t) w_{uv} |u\rangle\langle v|, \qquad f_{uv}(t) = f_{vu}^*(t).$$

The graph G from which H_G is derived will be called the *interaction graph*, which restricts the allowed interactions in H_G.

In this definition of the control Hamiltonian, we assume arbitrary time-dependent control over each allowed interaction, by tuning the *controls* $f_{uv}(t)$. In the following, we assume that the controls $f_{uv}(t)$ are continuous functions of time, as required for adiabatic evolution. Moreover, to avoid dealing with quickly oscillating laser fields, we assume that an appropriate rotating frame is considered and that off-resonant fields are neglected through a rotating wave approximation. This is important later, as multiple f_{uv} should not become 0 simultaneously. Hence, each $f_{uv}(t)$ should be a slowly changing function of time, representing, for example, the envelope of a laser's amplitude.

Thanks to the mapping to graphs, we can use various notions from graph theory. We denote with $G - v$ the graph G in which the vertex v and all the edges incident to v are removed.

Definition 1. A *bipartite graph* has a vertex set V, which can be separated into two independent subsets V_1, V_2 such that each edge $uv \in E$ must run *between* V_1 and V_2 (that is, $u \in V_1$ and $v \in V_2$ or vice versa).

A *semi-bipartite graph with parts* V_1 *and* V_2[31,32] is a bipartite graph in which edges within V_2 are allowed (including self-loops), but edges within V_1 are still prohibited. For example, the graph in Fig. 1 is semi-bipartite with $V_1 = \{|1\rangle, |3\rangle\}$, but not bipartite unless $\varepsilon = 0$.

Note that for a connected bipartite graph, the decomposition $V = V_1 \sqcup V_2$ is determined uniquely (up to interchanging V_1 and V_2), while this is almost never the case for semi-bipartite graphs: any vertex in V_1 may be moved to V_2. Hence, the decomposition is an essential part of the data. However, for our results, we want to take $|V_1| = |V_2| + 1$, which means that we cannot easily move points from V_1 to V_2.

We let $\mathcal{V}$ denote the vector space spanned by the states $|v\rangle$ corresponding to the vertices v in V. Likewise, we use $\mathcal{V}_1, \mathcal{V}_2$ to denote the subspaces corresponding to subsets V_1, V_2. We order the basis of $\mathcal{V}$ by first stating the elements of $\mathcal{V}_1$ and then the elements of $\mathcal{V}_2$. In this basis, the interaction graph has the form

$$A_G = \begin{pmatrix} 0 & B \\ B^T & C \end{pmatrix}, \tag{3}$$

where B is a matrix of size $|V_1| \times |V_2|$ and C has size $|V_2| \times |V_2|$. We will mostly use this form of A_G throughout this work.

Definition 2. We use *commensurate couplings* to denote the choice of couplings $f_{uv}(t)$ such that

$$\begin{aligned} f_{vu}(t) &= f_v(t), && \forall\, u \in V_2, v \in V_1, \\ f_{vu}(t) &= 1, && \forall\, u, v \in V_2. \end{aligned}$$

In other words, for each vertex $v \in V_1$, the incident couplings are changed proportionally, whereas all couplings within V_2 have to be equal to one.

Note that because we consider semi-bipartite graphs, the above definition covers the controls for all edges. In such cases, with the interaction graph given in the form of Eq. (3), we may write

$$H_G(t) = F(t) A_G F^*(t), \tag{4}$$

where $F(t) = \mathrm{diag}(f_1(t), \ldots, f_{|V_1|}(t), 1, \ldots 1)$.

We are now ready to state our main result. Consider a set of parties (vertices) $P \subseteq V_1$ located on a graph, who want to send a quantum state to each other. This turns out to be possible with a control Hamiltonian H_G, under certain graph restrictions, as made precise below.

Theorem 3. *Let $G = (V, E, w)$ be a connected, weighted, semi-bipartite graph with parts V_1 and V_2. Let $P = \{p_j\}_{j=1}^k \subseteq V_1$. We assume that*

1. $|V_1| = |V_2| + 1$.
2. *Either of the following:*

2a. *For all p_j, $\det(A_{G-p_j}) \neq 0$.*
2b. *A_G has a unique zero eigenvector, which has nonzero amplitude on each p_j.*

Then, for any $a, b \in P$, the following choice of commensurate couplings are such that $H_G(t)$ adiabatically transfers amplitude from a to b in total time T:

$$\begin{aligned} &f_a(0) = 0, \\ &f_b(T) = 0, \\ &f_v(t) \neq 0 \text{ for all } v \notin P, \\ &\text{no two } f_v(t) \text{ may be zero simultaneously.} \end{aligned} \tag{5}$$

Hence, the system exhibits a unique, continuously changing zero eigenstate, which is localized at a for $t = 0$ and at b for $t = T$.

Before we prove this theorem, we would like to analyze the statement. The proof is given after Remark 7.

The main importance of Theorem 3 is that there exist large classes of graphs that allow state transfer under a generalized form of the counter-intuitive pulse sequence encountered in STIRAP. Equation (5) allows abundant freedom in the choice of controls, although the theorem does not say anything about which controls are *optimal* (in the sense that they result in the smallest adiabatic error for a fixed time T). It also does not say anything about the reliability of the control protocol or about the size of the energy gap (except that it is non-zero). We numerically address gap size and transfer fidelities as a function of graph size in Sec. VI.

We also note that Eq. (5) is not exhaustive: there may be a wider class of controls that guarantees state transfer under our assumptions. On the other hand, even if assumptions 1 and 2 of Theorem 3 are satisfied, the controls cannot be *any* function of time: for any nontrivial graph G there exist controls f_{uv} that cause H_G to have a degenerate zero eigenvalue (an example is the case where too many f_{uv} become 0). We leave investigating the tightness of our results as an open problem.

Remark 4. For practical purposes, the only couplings f_{uv} that actually *require* time-dependent control are those directly connected to sender and receiver; controlling any of the other couplings is optional. In fact, the control procedure can be performed locally and sequentially: it is possible to first only change the controls near a and then only those near b. An example is the choice

$$f_v(t) = \begin{cases} \min\{2t/T, 1\}, & v = a \\ \min\{1 - 2t/T, 1\}, & v = b \\ 1, & \text{else.} \end{cases}$$

In particular, the receiver, b, can be chosen after the process has been initialized.

Remark 5. As seen in the proof, assumptions 1 and 2 are chosen precisely such that the Hamiltonian $H_G(t)$ has exactly one zero eigenvalue at all times. We show that this gives a non-zero gap, bounded from below uniformly over time.

Also note that in the physics literature, the gap is often addressed in the limit of increasing system size, whereas we assume that a graph has a fixed, finite size.

Assumption 2 is not very intuitive. Therefore, we will give two approaches to attaining it in Sec. V, one via perfect matchings, and one reducing graphs by cutting dangling vertices.

Assumptions 2a and 2b are equivalent under assumption of 1. More precisely, the following proposition holds:

Proposition 6. Let $G = (V, E, w)$ be a weighted, semi-bipartite graph with parts V_1 and V_2 such that $|V_1| = |V_2| + 1$, and let $p \in V_1$. Then, the following are equivalent:

a. $\det(A_{G-p}) \neq 0$.
b. *A_G has a unique zero eigenvector, which has non-zero amplitude on p.*

Proof. Let us first show that, thanks to $|V_1| = |V_2| + 1$, there must exist a zero-energy eigenvector $|z\rangle = (z_1, 0) \in \mathcal{V}_1$ whose nonzero amplitudes z_1 are only located on sites in V_1. This holds because in the eigenvalue equation, using the form of Eq. (3),

$$\begin{pmatrix} 0 & B \\ B^T & C \end{pmatrix} \begin{pmatrix} z_1 \\ 0 \end{pmatrix} = \begin{pmatrix} 0 \\ B^T z_1 \end{pmatrix} = 0,$$

the system of equations $B^T z_1 = 0$ has $|V_1|$ variables and $|V_2|$ constraints; hence, it must always have at least one non-trivial solution.

We start with the implication from a to b. By the previous argument, the rank of A_G can be at most $|V| - 1$. However, as $\det(A_{G-p}) \neq 0$, the submatrix A_{G-p} must be of maximal rank, which is also $|V| - 1$. As the rank of a submatrix gives a lower bound on the rank of a matrix, this shows that $\mathrm{rk} A_G \geq |V| - 1$. Therefore, there is a unique zero eigenvector.

Let this eigenvector be v; let its component at p be v_p and its components away from p be $\widetilde{v}$ (so $\widetilde{v}$ is a vector with $|V| - 1$ components). We can write A_G as a block matrix,

$$A_G = \begin{pmatrix} 0 & b_p \\ b_p^T & A_{G-p} \end{pmatrix},$$

where we wrote the component corresponding to p as the first component for simplicity. As v is a zero eigenvector, we get

$$0 = A_G v = \begin{pmatrix} 0 & b_p \\ b_p^T & A_{G-p} \end{pmatrix} \begin{pmatrix} v_p \\ \widetilde{v} \end{pmatrix} = \begin{pmatrix} b_p \widetilde{v} \\ b_p^T v_p + A_{G-p} \widetilde{v} \end{pmatrix}.$$

If $v_p = 0$, then $\widetilde{v} \neq 0$, as an eigenvector cannot be zero, but then $A_{G-p}\widetilde{v} \neq 0$, as $\det(A_{G-p}) \neq 0$. This is a contradiction, so we must have $v_p \neq 0$.

Now, we prove the implication from b to a by counterpositive. Hence, we assume $\det(A_{G-p}) = 0$ and show that there exists a zero eigenvector of A_G whose p-component is zero. Again, for notational simplicity, we write the component corresponding to p as the first component, so we have

$$A_G = \begin{pmatrix} 0 & B \\ B^T & C \end{pmatrix} = \begin{pmatrix} 0 & 0 & b_p \\ 0 & 0 & \widetilde{B} \\ b_p^T & \widetilde{B}^T & C \end{pmatrix}.$$

From this, we get

$$A_{G-p} = \begin{pmatrix} 0 & \widetilde{B} \\ \widetilde{B}^T & C \end{pmatrix},$$

where, crucially, the sizes of $\widetilde{B}$ and C are equal by the assumption $|V_1| = |V_2| + 1$. Hence,

$$\det(A_{G-p}) = \pm \det(\widetilde{B}\widetilde{B}^T) = \pm \det(\widetilde{B})^2.$$

Now, by assumption $\det(A_{G-p}) = 0$, so $\det(\widetilde{B}^T) = 0$. Therefore, there exists a zero eigenvector u of $\widetilde{B}^T$. If we define $v = (0, u, 0)$, then

$$A_G v = \begin{pmatrix} 0 & 0 & b_p \\ 0 & 0 & \widetilde{B} \\ b_p^T & \widetilde{B}^T & C \end{pmatrix} \begin{pmatrix} 0 \\ u \\ 0 \end{pmatrix} = \begin{pmatrix} 0 \\ 0 \\ \widetilde{B}^T u \end{pmatrix} = 0,$$

so we have constructed a zero eigenvector of A_G with zero amplitude on p, giving a contradiction. □

Remark 7. In fact, the implication from a to b goes through even in the case, G is not semi-bipartite; the proof does not use this assumption. However, for the other direction, it is essential.

Proof of Theorem 3. By the first part of the Proof of Proposition 6, there exists a zero-energy eigenvector $|z\rangle$ for any choice of controls.

By construction, the couplings $f_{uv}(t)$ in Eq. (5) are such that at times 0 and T, the respective states $|a\rangle$ and $|b\rangle$ are zero-energy eigenstates. We will argue that, using the given control scheme, the zero-energy subspace is one-dimensional at all times.

When all controls f_v are equal to one, then $H_G = A_H$ and the zero-energy eigenstate $|z\rangle$ is unique, by assumption 2.

When the couplings change commensurately, but remain non-zero, the eigenstate $|z\rangle$ changes as

$$|z(t)\rangle \propto F(t)^{-1}|z\rangle, \tag{6}$$

as can be seen from Eq. (4). Because F is diagonal, $|z(t)\rangle$ is still located on V_1. It is unique because given any zero eigenvector $|w\rangle$ of $H_G(t)$, $F(t)|w\rangle$ is an eigenvector of A_G and, hence, must be equal, up to scaling, to $|z\rangle$.

Special care has to be taken when reducing weights to zero. When reducing $f_p (p \in P)$ toward zero, assumption 2a guarantees that no zero eigenvectors occur on $G - p$, hence $|p\rangle$ must then be the unique zero eigenstate. This shows that any controls f_v satisfying Eq. (5) indeed pertain a unique zero-energy eigenstate and provide the correct initial and final state at times $t = 0$ and $t = T$.

Because the graph is finite, there are also finitely many eigenvalues for each t, and by the above, exactly one of them equals zero. Therefore, there must be a non-zero gap around zero for any fixed t. Furthermore, the interval $[0, T]$ is compact, and the eigenvalues and the gap depend continuously on the time, and so the gap must achieve its infimum at some $t_0 \in [0, T]$. Hence, this gap can be bounded uniformly by the gap at t_0, a positive number ε, which then bounds the A_k from Eq. (1). This shows that we can use the adiabatic theorem to find that a sufficiently high protocol time T allows state transfer at arbitrary accuracy. □

The unique zero-eigenstate $|z(t)\rangle$ has many favorable stability properties. Its eigenvalue is *exactly* 0 throughout the whole protocol, independent of changes to w_{uv}, as long as the graph remains semi-bipartite. The constant energy makes the state's dynamical phase easy to track. Moreover, it has exactly 0 amplitude on $\mathcal{V}_2$, which makes it insensitive to any decoherence on sites in V_2. The state $|z\rangle$ generalizes the "dark state" of conventional STIRAP and CTAP, inheriting important features that make these protocols attractive for practical purposes.

One might be concerned that, when reducing all controls $f_{p_j v}$ incident to a certain party p_j to zero, it is hard to maintain the commensurate ratios between the couplings. Fortunately, it turns out that in such cases, commensurateness is not essential: the condition $\det(A_{G-p_j}) \neq 0$ guarantees that the zero eigenstate remains unique as long as all other sites remain commensurately coupled. This holds because the rank of A_G must be at least that of A_{G-p_j}, which shows that for *any* couplings between p_j and the rest of the graph, there can be at most one zero-energy state. This freedom gives the protocol a convenient stability to imperfect controls.

The time scale T required by the protocol is determined by the gap in the spectrum around the zero eigenvalue, as opposed to the well-studied gap between the lowest and second lowest energy.[33] To our best knowledge, little is known about the gap around zero, and characterizing its scaling is an interesting open problem. In Sec. VI, we numerically study the scaling for certain example graphs.

IV. APPLICATIONS

Our main result requires a physical system to obey our conventions of control Hamiltonian H_G for certain graphs G with sufficiently flexible controls f_{uv}. The mathematical framework we consider applies to various realistic cases, such as

- Discrete energy levels coupled by (near-)resonant laser fields, like electronic levels in atoms or molecules, such as typically considered in STIRAP.[2] The lasers can also be off-resonant, as long as each state in V_2 has all of its incident couplings at the same off-resonance. Either way, a transformation to the interaction picture and assumption of the rotating wave approximation are required.
- Systems where a quantum particle "hops" between coupled sites, such as electrons caught in quantum dots,[17,34] or atoms or atomic condensates trapped in optical potentials.[16,35,36]
- An XX-model of interacting spins of the form

$$H_{\mathrm{XX}} = \frac{1}{2}\sum_{uv\in E} w_{uv}(X_u X_v + Y_u Y_v) + h\sum_{u\in V} Z_u,$$

  where $\{X_u, Y_u, Z_u\}$ are the Pauli matrices acting on the site u in the sector with a single spin excitation.[18]

The most interesting application might be in quantum information processing. Note that our protocols can transmit quantum information, for example, when the transported state represents the position of a quantum particle with internal degrees of freedom, as is the case with CTAP, or when a superposition between a shared vacuum and an excitation on a graph may be made. The latter applies to the XX-model, where an initial state of the form

$$|\psi(0)\rangle = \alpha|0\rangle_a|0\ldots0\rangle + \beta|1\rangle_a|0\ldots0\rangle$$

can be initialized locally at site a. The first term is an eigenstate of H_{XX} and does not change. The second term evolves in an invariant subspace spanned by states with a single spin excitation. The evolution is then described by a Hamiltonian of the form H_G, allowing the spin excitation to be transferred to some other location b.

In the context of information transfer, care has to be taken with the additional phase that is picked up throughout the protocol. As an example, in the XX model described above, the single-excitation subspace amplitude β picks up a relative phase $\beta \to e^{-ihT}\beta$ relative to the vacuum amplitude α. Moreover, the transfer protocol itself gives an additional phase to the transferred excitation, as previously observed by Ref. 24. This becomes relevant when dealing with the XX model or when transporting entangled particles or states. Owing to Eq. (6), as long as $f_{uv}(t)$ remain real-valued, the additional phase acquired by the state when transferring from site a to b is equal to $\arg(z_a/z_b)$, where z_a, z_b are elements of the zero-eigenvector $|z\rangle$ of A_G. Hence, for some applications, this vector may need to be explicitly calculated once.

As a potential realistic application, Ref. 37 observed that individual quantum processors based on quantum dots are limited in size, increasing the need for communication between nearby processors. Our results readily generalize the CTAP protocol[17] to transfer electrons through a network of quantum dots, and the possibility to use more general graphs may be of great benefit for larger quantum computer architectures.

Another new application is in a delayed transfer scheme, previously addressed in Ref. 38. The sender a can initialize the system into the dark state $|z\rangle$ and leave it at that such that any party in P can retrieve the quantum state, at any time they like. This opens the possibility to share unclonable quantum information among many parties without yet knowing which party is required to obtain the information.

V. EXAMPLES OF VIABLE GRAPHS

The main assumptions of Theorem 3, especially requirement 2, may not be very intuitive but can be guaranteed in certain cases. In this section, we present two results in this direction. First, we discuss a procedure to generate viable graphs by iteratively adding or removing dangling vertices. Next, we show that for any graph that allows, for each p_j, a perfect matching when a party p_j is removed, our assumptions are satisfied with probability 1 when the weights w_{uv} are chosen at random.

A. Adding and removing vertex pairs where one is dangling preserves the nullity

Consider a setting where one knows a graph G and a set of parties P that satisfy the assumptions of Theorem 3. One may now extend the graph by connecting first a vertex u in an arbitrary way and then connecting a vertex v only to u. It turns out that, for any choice of non-zero weights, the number of zero eigenvectors does not change in this process.

We make this precise as follows: For an $(n \times n)$-matrix A, let $\eta(A) = n - \mathrm{rk}(A)$ denote the nullity of the matrix.

Lemma 8. Let G be a graph with a vertex v of degree 1 whose unique neighbor is u ($u \neq v$). Then,

$$\eta(A_G) = \eta\left(A_{G-\{v,u\}}\right).$$

Proof. Let $\widetilde{G}$ denote the graph $G - \{v, u\}$. Assuming for convenience that v and u are the first and second columns of the adjacency matrix A_G, respectively, we can write

$$A_G = \begin{pmatrix} 0 & w_{uv} & 0 \\ w_{vu} & w_{uu} & b \\ 0 & b^T & A_{\widetilde{G}} \end{pmatrix}.$$

We can write any vector $|z\rangle$ as $(z_v, z_u, \widetilde{z})$. Now, $w_{uv} \neq 0$ and

$$0 = A_G|z\rangle = \begin{pmatrix} 0 & w_{uv} & 0 \\ w_{vu} & w_{uu} & b \\ 0 & b^T & A_{\widetilde{G}} \end{pmatrix} \begin{pmatrix} z_v \\ z_u \\ \widetilde{z} \end{pmatrix} = \begin{pmatrix} w_{uv} z_u \\ w_{vu} z_v + w_{uu} z_u + b \cdot \widetilde{z} \\ b^T z_u + A_{\widetilde{G}} \widetilde{z} \end{pmatrix},$$

implying that $z_u = 0$, and hence, also $z_v = -\frac{1}{w_{vu}} b \cdot \widetilde{z}$ and $A_{\widetilde{G}} \widetilde{z} = 0$. Hence, we get a linear isomorphism $\ker A_G \to \ker A_{\widetilde{G}} : (z_v, z_u, \widetilde{z}) \mapsto \widetilde{z}$ with inverse $\widetilde{z} \mapsto (-\frac{1}{w_{vu}} b \cdot \widetilde{z}, 0, \widetilde{z})$. As the nullity is the dimension of the kernel, this shows $\eta(A_G) = \eta(A_{\widetilde{G}})$. □

Note that in Lemma 8, we did not require the assumption of semi-bipartiteness, although the latter is still required for our adiabatic protocol. We obtain the following corollary:

Corollary 9. Suppose that G is a semi-bipartite graph with parts V_1 and V_2 such that $|V_1| = |V_2| + 1$. Fix a set of parties $P \subseteq V_1$. Suppose that v is a dangling vertex, $v \notin P$, whose unique neighbor is u. Then, condition 2 of Theorem 3 holds for G if and only if it holds for $G - \{u, v\}$.

Proof. Recall that one of the two equivalent statements of condition 2 is that $\det(A_{G-p_j}) \neq 0$ for all $p_j \in P$. Let us first assume that G satisfies this condition. Because $\det(A_{G-p_j}) \neq 0$, the nullity of A_{G-p_j} is non-zero. By Lemma 8, the nullity of $A_{G-\{u,v\})-p_j}$ is also non-zero; hence, it has a non-zero determinant and thus satisfies condition 2a as well. The same reasoning also proves the other direction. □

Corollary 9 shows that new viable graphs can be generated by adding or removing vertices from the existing graphs that are already known to satisfy the assumptions of Theorem 3. When adding vertices, one may first connect a vertex u in *any* way, as long as the semi-bipartiteness is not violated, and then attach a vertex v only to u. When removing vertices, one must find a dangling vertex v and remove it together with its neighbor u, as long as the connectedness is preserved. On graphs generated this way, the requirements of Theorem 3 can be guaranteed.

When adding new vertices to a graph this way, it may also be possible to add the new vertices to the set of parties P, under the following conditions. It is never possible to add a vertex $u \in V_1$ to the set P when u is adjacent to a dangling vertex. For a new dangling vertex $v \in V_1$ that is to be added to the set P, assumption 2b requires that the zero eigenvector z of the new adjacency matrix has nonzero amplitude on v. From the Proof of Lemma 8, we see that we require $0 \neq z_v = -\frac{1}{w_{vu}} b \cdot \widetilde{z}$, where b is a vector containing the weights of u to the original vertices (excluding u and v) and $\widetilde{z}$ is the original zero eigenvector.

Below, we give two example of new families of graphs that allow adiabatic transfer. Various examples of viable graphs are also depicted in Fig. 2.

Example 10 (Subdivided trees). Let $T = (V_T, E_T)$ be any tree. We define the subdivided tree $\widetilde{T} = (V_{\widetilde{T}}, E_{\widetilde{T}})$ by replacing every edge by two edges and a vertex: the new vertex set $V_{\widetilde{T}} = V_T \sqcup E_T$ is given by the vertices and edges of T, and the edge set $E_{\widetilde{T}} = \{\{v, e\} : v \in V_T, e \in E_T, v \in e\}$ consists of edges that connect each vertex $v \in V_T$ to its incident edges $e \in E_T$. An example of such a subdivided tree is shown in Fig. 3. The decomposition $V_{\widetilde{T}} = V_T \sqcup E_T$ guarantees that $\widetilde{T}$ is a bipartite graph, and since T is a tree we find that the vertex classes satisfy $|V_T| = |E_T| + 1$. Moreover, we can iteratively remove leaves from the tree to reduce to a single vertex or single edge, showing that any $\widetilde{T}$ constructed this way satisfies the conditions of Theorem 3.

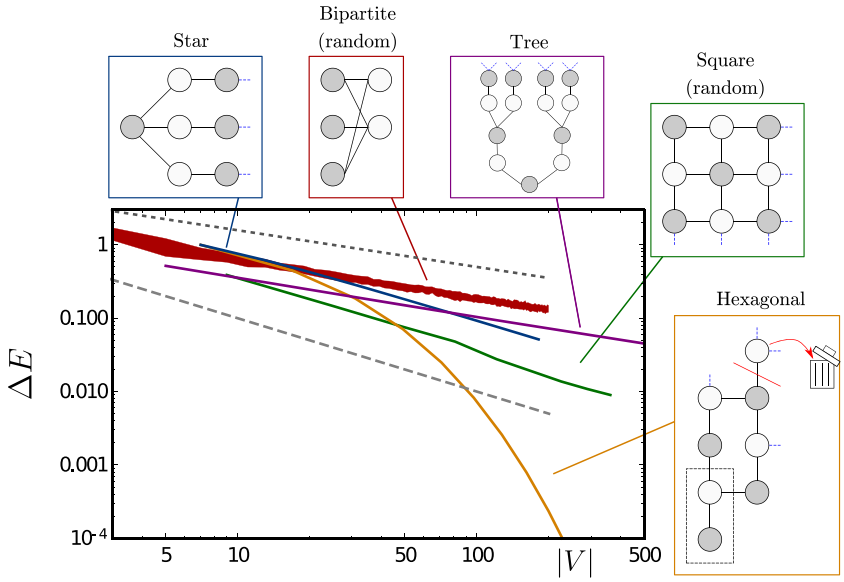

FIG. 2. Scaling of the eigenvalue gap ΔE between the unique zero eigenvalue and the closest other eigenvalue on a log-log scale. These are calculated for various bipartite graphs of various sizes $|V|$. The annotation (random) indicates that the weights were randomly chosen in the interval [0, 2] to guarantee a unique zero eigenvector. The lower dashed line indicates $\Delta E = 1/|V|$, and the upper dashed line follows $\Delta E = 10/\sqrt{|V|}$. Interestingly, for most of the graphs, we study that the gap decay scales proportionally to $1/|V|$ or better. Hexagonal grids are an exception, as these are found to decay superpolynomially. Reproduced with permission from Groenland, "Quantum protocols for few-qubit devices," ILLC Dissertation Series (University of Amsterdam, 2020).[43]

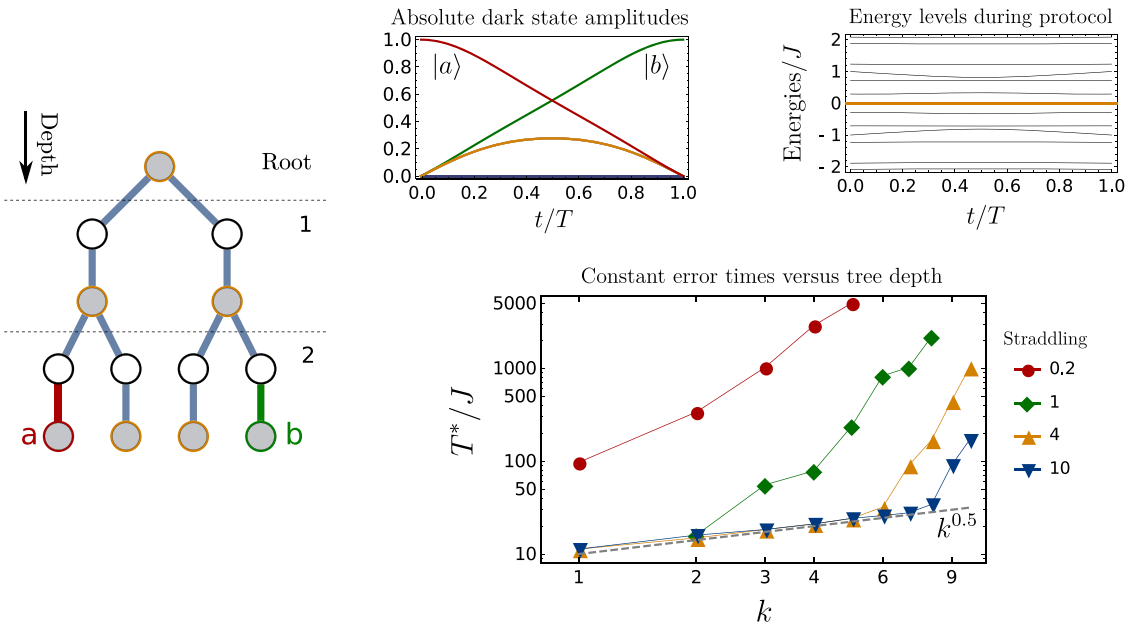

FIG. 3. Simulation results on tree graphs are presented. A tree of depth $k = 2$ is shown on the top-left, with receivers a and b maximally separated. The top-right shows the ideal state evolution over time and the energy levels during the protocol. The times T^* required for constant fidelity increase steeply with the exponential size $|V|$ of the graph (bottom), except when sufficiently strong straddling is applied, leading to $T^* \propto k^{0.5}$ (dashed line). Reproduced with permission from Groenland, "Quantum protocols for few-qubit devices," ILLC Dissertation Series (University of Amsterdam, 2020).[43]

Example 11 (Hexagonal grids). Hexagonal grids can be constructed from two-vertex unit cells that are all oriented in the same direction. These grids are bipartite, with each unit cell containing one vertex from V_1 and the other from V_2. If we start with a single vertex and keep attaching unit cells in a hexagonal grid pattern such that one of the newly attached vertices is dangling, then each of the grids constructed this way satisfies the conditions of Theorem 3.

B. Graphs with certain matchings make the protocol work almost surely

A *perfect matching* in a graph G is a set of disjoint edges that covers all the vertices. In this section, we show that on semi-bipartite graphs G where $G - \{p_i\}$ has a perfect matching for all i, taking arbitrary weights from a continuous distribution results in an interaction graph that satisfies the conditions of Theorem 3 with probability one. This gives another way to generate a large class of graphs on which the adiabatic transfer protocol works.

Theorem 12. *Let $G = (V, E, w)$ be a weighted semi-bipartite graph with parts V_1 and V_2 where $|V_1| = |V_2| + 1$. Let $P = \{p_j\}_{j=1}^{k} \subseteq V_1$. Suppose that for all i, there exists a perfect matching in $G - p_i$. Then, if weights w_{uv} are chosen randomly from a continuous distribution (meaning that no value has positive probability) for all $uv \in E$, we find $\det(A_{G-p_j}) \neq 0$ for all p_j with probability 1.*

Note that the theorem exactly gives us condition 2a required by the protocol.

Proof. It suffices to prove that $\det(A_{G-p_i}) \neq 0$ with probability 1 for a fixed $i \in \{1, \ldots, k\}$; the claim of the theorem then follows since a countable intersection of events with probability 1 still has probability 1.

Let $p = p_i$ be given. We will first permute the rows and columns of the matrix A_{G-p} to bring it in a convenient form; such a permutation only affects the determinant of the matrix by a sign, which is irrelevant to us.

By assumption, there is a perfect matching on the graph $G - p$. Since $|V_1 \backslash \{p\}| = |V_2|$ and there are no edges within V_1, any perfect matching must use only edges between V_1 and V_2. Let $u_1v_1, \ldots, u_kv_k \in E \cap (V_1 \times V_2)$ denote the edges given in a perfect matching on $G - p$. Permute the rows and columns such that the rows are in the order $u_1, v_1, u_2, v_2, \ldots$ and the columns are in the order $v_1, u_1, v_2, u_2, \ldots$. We show with an inductive argument that for all $\ell \in \{1, \ldots, k\}$, the matrix A_ℓ on the first 2ℓ rows and columns has non-zero determinant with probability 1. This proves the claim.

For $\ell = 1$, we consider

$$\det\begin{pmatrix} w_{u_1v_1} & 0 \\ w_{v_1v_1} & w_{u_1v_1} \end{pmatrix} = w_{u_1v_1}^2,$$

since $w_{u_1u_1} = 0$ as $u_1 \in V_1$. As $w_{v_1v_1}$ is sampled uniformly at random from $[0, 1]$, this is non-zero with probability 1. Now suppose we have shown the statement up to some ℓ. We find

$$\det\begin{pmatrix} A_\ell & b_1 & b_2 \\ d_1 & w_{u_{\ell+1}v_{\ell+1}} & 0 \\ d_2 & w_{v_{\ell+1}v_{\ell+1}} & w_{u_{\ell+1}v_{\ell+1}} \end{pmatrix} = \det(A_\ell) w_{u_{\ell+1}v_{\ell+1}}^2 + b w_{u_{\ell+1}v_{\ell+1}} + c$$

for some b and c, which do not depend on $w_{u_{\ell+1}v_{\ell+1}}$, and where we may assume that $\det(A_\ell) \neq 0$. Since the other entries do not depend on $w_{u_{\ell+1}v_{\ell+1}}$ and this gets sampled independently of the other entries, we may view $\det(A_\ell)$, b and c as constants. Since there are at most two possible values in $[0, 1]$, which make a quadratic polynomial $ax^2 + bx + c$ equal to zero (if $a \neq 0$), with probability 1 the expression will be non-zero. Continuing until $\ell + 1 = k$, we conclude $\det(A_{G-p}) \neq 0$ with probability 1 as desired. □

Remark 13. From the proof, it follows that the assumptions in Theorem 12 can be relaxed: the requirement that the weights are chosen from a continuous distribution is only necessary for the edges involved in the matching.

In fact, it is possible to show that the adjacency matrix of G is equivalent to a matrix with non-zero entries on the diagonal if and only if there is a perfect matching. Limited generalization is also possible to non-bipartite graphs.

The Proof of Theorem 12 also suggests a (weak) lower bound on the determinant $\det(A_{G-p_i})$ with some probability and hence on the eigenvalue gap of A_G. We elaborate on this in Appendix A.

VI. NUMERICS

Our main result in Theorem 3 states merely that adiabatic transfer is possible at *some* time scale to which we remained agnostic. Particularly, the randomly weighted graphs with perfect matchings in Sec. V B potentially give rise to configurations with a very small energy gap, giving rise to long transfer times T. An in-depth study of the gap between the zero eigenvalue and the next on semi-bipartite graphs is left as

an open problem, but to give *some* indication of the quantitative behavior of our protocol, we resort to numerics. First, we calculate the scaling of the energy gap for various graphs. After that, we consider the fidelity of transfer in subdivided trees of various depths.

Figure 2 depicts the scaling of the energy gap around the zero energy state, as a function of the number of vertices $|V|$, for various types of graphs. For most graphs, we consider the unweighted versions, setting $w_{uv} = 1$ whenever the corresponding edge is present. Some graphs have the annotation "random," which means that the graphs typically do not have a unique zero eigenvalue when all weights equal one; we then ensure a unique zero eigenvector by multiplying each weight w_{uv} with a random number chosen independently and uniformly chosen between 0 and 2. We took the average energy gap over 50 such perturbations. The precise details of the specific graphs we generated can be found in Appendix B.

These results show that the energy gap often decays roughly as $\Delta E \propto |V|^{-1}$ or better, similarly to conventional STIRAP over a linear chain, with hexagonal grids being an exception.

To assess the actual accuracy of our protocol, we numerically simulate the time evolution of a transferred state. As graphs, we choose *binary* trees of depth k, as these allow transfer between a large number of parties. To guarantee that requirement 1 is always fulfilled, we use the subdivision procedure in Example 10, putting a vertex on each edge. This leads to a graph as shown in Fig. 3. The possible communicating parties P are chosen to be the leaves (endpoints) of the tree, allowing $|P| = 2^k$ parties to be connected. The actual transfer takes place between parties a and b, which are at maximum distance from each other.

We define the transfer error as $\mathcal{E} = 1 - |\langle b|U_T|a\rangle|$, where U_T denotes the unitary time-evolution operator as found by numerically solving Schrödinger's equation and T is the total protocol's time. We choose simple time-dependent couplings $f_a = Jt/T$ and $f_b = J(1 - t/T)$, while all other controls remain $f_v = 1$. Moreover, we define T^* as the lowest time for which $\mathcal{E} < 0.05$, setting a bar for transfer with 95% fidelity.

Owing to the exponentially large size $|V|$ of the graphs, the time required rapidly increases with k (Fig. 3). Interestingly, we find that the technique of straddling,[15,17] where all controls f_v except for f_a and f_b are multiplied by a factor s, flattens the scaling down to roughly $T^* \approx 10\sqrt{k}$, up to a certain k where the steep increase is observed again. Reference 39 already predicted a favorable scaling $T^* \propto \sqrt{n}$ for linear chains of length n in the strong straddling limit. It is surprising that here we find a similar scaling in k rather than n, even though the number of vertices increases exponentially in k.

There are various reasons to believe that the strong straddling scaling cannot remain valid for increasingly large systems, for example, due to Lieb–Robinson bounds.[40] Still, with a modest straddling factor $s = 10$, transfer at favorable scaling $T^* \propto \sqrt{\log(|P|)}$ is observed for graphs of up to 1000 sites, showing that near-term experiments can benefit from this effect.

VII. CONCLUSION

To summarize, we extend the set of graphs in which STIRAP-like protocols are known to work. The sufficient requirements are made precise in assumptions 1 and 2, which can be guaranteed using the techniques in Sec. V. We inherit the most important properties of the conventional protocols: the adiabatic controls do not require precise amplitudes or timings, the system's energy is *exactly* zero at all times, and the fidelity is largely insensitive to decay on sites in V_2. Various extensions, such as straddling and multi-party transfer, can be readily incorporated. In the studied example of tree-shaped graphs, we find that with mild straddling, the fidelities are much better than naïvely expected.

As our requirements are sufficient but not necessary, we would be interested to see that further work explores other graphs with unique zero eigenstates and gives guarantees on spectral gaps around the zero eigenvalue for specific graphs. Moreover, we look forward to seeing state-of-the-art experiments test our results in practice.

ACKNOWLEDGMENTS

We thank Andrew Greentree for inspiring discussion and Kareljan Schoutens for discussions and feedback on this manuscript. We also thank the anonymous referee for useful remarks on both the content and the presentation of the text. R.K. was supported by the VICI grant (No. 639.033.211) from the Netherlands Organization for Scientific Research and by the Max-Planck-Gesellschaft. K.G. was supported by the QM&QI grant from the University of Amsterdam, supporting QuSoft.

APPENDIX A: ON THE EIGENVALUE GAP AROUND 0

The eigenvalue gap between the ground state and the first excited state is an active field of research. The gap between a zero eigenvalue and the nearest non-zero eigenvalue seems to have received significantly less interest. Here, we present some thoughts that could be useful in characterizing the gap around 0: first, on estimating the determinant when weights of a perfectly matchable graph are chosen at random, and second, by using Cauchy's interlacing theorem of eigenvalues.

1. Robustness guarantees using the determinant

When weights w_{uv} are chosen from $[0, 1]$, all eigenvalues of A_G satisfy $|\lambda| \leq d_{\max}(G)$ for $d_{\max}(G)$ the maximum degree of G. Since the determinant is the product of the eigenvalues, this gives the lower bound $|\lambda| \geq \frac{\det(A_G)}{d_{\max}(G)^{n-1}}$ for a graph G on n vertices. Hence, the lower bound on the determinant of A_G also gives a lower bound on the smallest eigenvalue.

Moreover, a lower bound on the determinants $\det(A_{G-p_i})$ gives the robustness guarantee that our protocol will keep working even if the weights cannot be held exactly at the aimed value. More precisely, if $|\det(A_{G-p_i})| > \epsilon$ for some $\epsilon > 0$, then by continuity of the determinant, this remains true even if the entries of A_{G-v} (that is, the weights on the edges) get permuted by at most some δ. Since the determinant is a polynomial, we may expect δ to be of a similar scale to ϵ. This implies that the uniqueness of the zero eigenvector would be guaranteed even if the weights of the edges are slightly perturbed. Note that the weights on the edges adjacent to p_i do not affect the determinant at all.

The Proof of Theorem 12 extends to give a weak lower bound on the determinant.

Theorem 14. *Let G be a semi-bipartite graph on parts V_1 and V_2 with a perfect matching $u_1v_1, \dots, u_\ell v_\ell$. Suppose that the weights on some edges of G, including the $w_{u_iv_i}$, are chosen independently and uniformly at random from $[0,1]$. Then, with probability at least $(\frac{1}{2})^\ell$, we have $|\det(A_G)| > (\frac{1}{2})^{3\ell-1}$.*

Proof. We may assume that there are no edges within V_1. (This assumption can be left out but makes the analysis easier.) As in the Proof of Theorem 12, we reorder the columns to $u_1, v_1, u_2, v_2, \dots$ and the rows to $v_1, u_1, v_2, u_2, \dots$ and prove the claim for all submatrices A_ℓ spanned by the first 2ℓ rows and columns for all $\ell \in \{1, \dots, k\}$.

The statement is true for $\ell = 1$: $\det(A_1) = w^2_{u_1v_1} > \frac{1}{4}$ with probability at least $\frac{1}{2}$. Suppose now that $|\det(A_\ell)| \geq \left(\frac{1}{2}\right)^{3\ell-1}$ with probability at least $\left(\frac{1}{2}\right)^\ell$ for some ℓ. Again, we find that

$$\det\begin{pmatrix} A_\ell & b_1 & b_2 \\ d_1 & w_{u_{\ell+1}v_{\ell+1}} & 0 \\ d_2 & w_{v_{\ell+1}v_{\ell+1}} & w_{u_{\ell+1}v_{\ell+1}} \end{pmatrix} = \det(A_\ell) w^2_{u_{\ell+1}v_{\ell+1}} + b w_{u_{\ell+1}v_{\ell+1}} + c$$

takes the form $ax^2 + bx + c$, where a, b, c do not depend on $x = w_{u_{\ell+1}v_{\ell+1}}$ and can hence be viewed as constants by the independence assumption. By the induction hypothesis, $|a| \geq \left(\frac{1}{2}\right)^{3\ell-1}$ with probability at least $\left(\frac{1}{2}\right)^\ell$.

We can rewrite $ax^2 + bx + c = a(x + b')^2 + c'$ for possibly different values b', c'. Then, $|a(x + b')^2 + c'| \leq \left(\frac{1}{2}\right)^{3(\ell+1)-1}$ if and only if $a(x + b')^2 \in \left(-c' - \left(\frac{1}{2}\right)^{3(\ell+1)-1}, -c' + \left(\frac{1}{2}\right)^{3(\ell+1)-1}\right)$. The probability of this happening is maximized when $b' = -\frac{1}{2}$, $|c'| = \left(\frac{1}{2}\right)^{3(\ell+1)-1}$ and the sign of c' and a is different; we may assume $a > 0$ as the other case is analogous. In this case, the interval is $\left(0, 2\left(\frac{1}{2}\right)^{3(\ell+1)-1}\right) = \left(0, \left(\frac{1}{2}\right)^{3\ell+1}\right)$. We find $a \geq \left(\frac{1}{2}\right)^{3\ell-1}$ with probability at least $\left(\frac{1}{2}\right)^\ell$ in which case independently with probability $\frac{1}{2}$ we have $|x + b'| \geq \frac{1}{2}$. Hence, with probability at least $\left(\frac{1}{2}\right)^{\ell+1}$, we find

$$a(x + b')^2 \geq \left(\frac{1}{2}\right)^{3\ell-1}\left(\frac{1}{2}\right)^2 = \left(\frac{1}{2}\right)^{3\ell+1} \notin \left(0, \left(\frac{1}{2}\right)^{3\ell+1}\right).$$

□

We cannot hope to do much better than the result above. Consider the case in which $A = \operatorname{diag}(a_1, a_1, \dots, a_k, a_k)$ is a diagonal matrix such that $\det(A) = a_1^2 \cdots a_k^2$ where the a_i get chosen independently and uniformly at random. Using the law of large numbers or the central limit theorem and the fact that $-\log(U(0,1)) \sim \operatorname{Exp}(1)$, it follows that $a_1 \cdots a_k$ is concentrated around $\left(\frac{1}{e}\right)^k$. In fact, one can prove using Chernoff bounds[41] that

$$\mathbb{P}\left(a_1 \cdots a_k \geq \left(0.5^{2/3}\right)^k\right) \leq e^{-(1/144)k}.$$

Hence, without further assumptions, we cannot hope to improve the exponential decay in the lower bound of the theorem.

2. Interlaced eigenvalues

We can obtain a lower bound on the eigenvalue gap using the following result, which follows from the fact that A_{G-p} is a principal submatrix of A_G.[42]

Theorem 15 (Cauchy interlacing theorem). *Let G be a graph with a vertex p. Let $\lambda_1 \leq \cdots \leq \lambda_{n+1}$ be the eigenvalues of A_G and $\mu_1 \leq \cdots \leq \mu_n$ the eigenvalues of A_{G-p}. Then,*

$$\lambda_1 \leq \mu_1 \leq \lambda_2 \leq \mu_2 \leq \cdots \leq \lambda_n \leq \mu_n \leq \lambda_{n+1}.$$

In our setup, one of the λ_i will be equal to 0, and the theorem shows that the gap to the second absolutely smallest eigenvalue is at least $\min_i|\mu_i|$, and hence, the eigenvalue gap

$$\Delta(G) \geq \max_{p \in V_1} \min_{\mu \text{ eigenvalue of } G-p} |\mu|.$$

Along with a bound on $\det(A_{G-p})$, as considered in Sec. V B, we can use this to obtain a lower bound on the eigenvalue gap of G. This bound is very weak, and based on the experiments in Sec. VI, it is our expectation that vastly better bounds can be obtained.

APPENDIX B: DETAILS OF THE NUMERICAL DIAGONALIZATION

The details of our numerics on the gap scaling for various graphs are as follows:

We generate *star graphs* by connecting k "arms," linear chains of length m, to a single center vertex. Interestingly, the eigenvalue gaps do not change as the number of arms increases. We fix the number of arms to 3 and vary the chain lengths to make larger graphs.

The *hexagonal grids* consist of unit cells of size 2. We take k^2 copies of these unit cells and place them on a $k \times k$ square grid, which is connected as indicated in Fig. 2. To enforce an odd number of sites, we remove a single site in the top-right corner, leading to $2k^2 - 1$ sites in total. Interestingly, the hexagonal grids are the only graph configuration we considered whose gap decays superpolynomially (yet slower than an exponential). Randomly perturbing weights does not change this behavior.

The *square grids* are chosen to have k by k vertices, where k is an odd number.

The *bipartite graphs* consist of two parts of size $m + 1$ and m, respectively. Each potential edge which can be laid to connect the two parts is added with probability $p = 0.81$. Because these graphs are also random for each data point, we also averaged the gap size over 50 random instantiations of the edge set. The thickness of the line indicates the standard deviation.

Finally, the subdivided binary *trees* are generated as in the main text: starting from a complete binary tree of certain depth, we create an additional vertex on each edge, which makes sure that $|V_1| = |V_2| + 1$.

DATA AVAILABILITY

The data that support the findings of this study are available from the corresponding author upon reasonable request.

REFERENCES

[1] U. Gaubatz, P. Rudecki, S. Schiemann, and K. Bergmann, "Population transfer between molecular vibrational levels by stimulated Raman scattering with partially overlapping laser fields. A new concept and experimental results," J. Chem. Phys. **92**, 5363–5376 (1990).
[2] N. V. Vitanov, A. A. Rangelov, B. W. Shore, and K. Bergmann, "Stimulated Raman adiabatic passage in physics, chemistry, and beyond," Rev. Mod. Phys. **89**, 015006 (2017).
[3] M. A. Kasevich, "Coherence with atoms," Science **298**, 1363–1368 (2002).
[4] K. Kotru, D. L. Butts, J. M. Kinast, and R. E. Stoner, "Large-area atom interferometry with frequency-swept Raman adiabatic passage," Phys. Rev. Lett. **115**, 103001 (2015).
[5] P. Král, I. Thanopulos, and M. Shapiro, "Colloquium: Coherently controlled adiabatic passage," Rev. Mod. Phys. **79**, 53–77 (2007).
[6] S. Stellmer, B. Pasquiou, R. Grimm, and F. Schreck, "Creation of ultracold Sr_2 molecules in the electronic ground state," Phys. Rev. Lett. **109**, 115302 (2012).
[7] D. Petrosyan, D. D. B. Rao, and K. Mølmer, "Filtering single atoms from Rydberg-blockaded mesoscopic ensembles," Phys. Rev. A **91**, 043402 (2015).
[8] S. A. Moses, J. P. Covey, M. T. Miecnikowski, D. S. Jin, and J. Ye, "New frontiers for quantum gases of polar molecules," Nat. Phys. **13**, 13–20 (2017).
[9] A. Ciamei, A. Bayerle, C.-C. Chen, B. Pasquiou, and F. Schreck, "Efficient production of long-lived ultracold Sr_2 molecules," Phys. Rev. A **96**, 013406 (2017).
[10] J. Pachos and H. Walther, "Quantum computation with trapped ions in an optical cavity," Phys. Rev. Lett. **89**, 187903 (2002).
[11] F. Troiani, U. Hohenester, and E. Molinari, "High-finesse optical quantum gates for electron spins in artificial molecules," Phys. Rev. Lett. **90**, 206802 (2003); arXiv:cond-mat/0304272.
[12] E. Paspalakis and N. J. Kylstra, "Coherent manipulation of superconducting quantum interference devices with adiabatic passage," J. Mod. Opt. **51**, 1679–1689 (2004).
[13] N. Timoney, I. Baumgart, M. Johanning, A. F. Varón, M. B. Plenio, A. Retzker, and C. Wunderlich, "Quantum gates and memory using microwave-dressed states," Nature **476**, 185–188 (2011).
[14] T. S. Koh, S. N. Coppersmith, and M. Friesen, "High-fidelity gates in quantum dot spin qubits," Proc. Natl. Acad. Sci. U. S. A. **110**, 19695–19700 (2013); arXiv:1307.8406.
[15] V. S. Malinovsky and D. J. Tannor, "Simple and robust extension of the stimulated Raman adiabatic passage technique to N -level systems," Phys. Rev. A **56**, 4929–4937 (1997).
[16] K. Eckert, M. Lewenstein, R. Corbalán, G. Birkl, W. Ertmer, and J. Mompart, "Three-level atom optics via the tunneling interaction," Phys. Rev. A **70**, 023606 (2004).
[17] A. D. Greentree, J. H. Cole, A. R. Hamilton, and L. C. L. Hollenberg, "Coherent electronic transfer in quantum dot systems using adiabatic passage," Phys. Rev. B **70**, 235317 (2004); arXiv:cond-mat/0407008.
[18] T. Ohshima, A. Ekert, D. K. L. Oi, D. Kaslizowski, and L. C. Kwek, "Robust state transfer and rotation through a spin chain via dark passage," arXiv:quant-ph/0702019 (2007).
[19] D. P. DiVincenzo and IBM, "The physical implementation of quantum computation," Fortschr. Phys. **48**, 771–783 (2000); arXiv:quant-ph/0002077.
[20] J. Preskill, "Quantum computing in the NISQ era and beyond," Quantum **2**, 79 (2018); arXiv:1801.00862.
[21] R. Menchon-Enrich, A. Benseny, V. Ahufinger, A. D. Greentree, T. Busch, and J. Mompart, "Spatial adiabatic passage: A review of recent progress," Rep. Prog. Phys. **79**, 074401 (2016).
[22] C. J. Bradly, M. Rab, A. D. Greentree, and A. M. Martin, "Coherent tunneling via adiabatic passage in a three-well Bose-Hubbard system," Phys. Rev. A **85**, 053609 (2012); arXiv:1201.6106.

[23]S. Longhi, "Coherent transfer by adiabatic passage in two-dimensional lattices," Ann. Phys. **348**, 161–175 (2014).
[24]A. D. Greentree, S. J. Devitt, and L. C. L. Hollenberg, "Quantum-information transport to multiple receivers," Phys. Rev. A **73**, 032319 (2006).
[25]B. Chen, W. Fan, Y. Xu, Y.-D. Peng, and H.-Y. Zhang, "Multipath adiabatic quantum state transfer," Phys. Rev. A **88**, 022323 (2013).
[26]C. Batey, J. Jeske, and A. D. Greentree, "Dark state adiabatic passage with branched networks and high-spin systems: Spin separation and entanglement," Front. ICT **2**, 19 (2015).
[27]J. R. Morris and B. W. Shore, "Reduction of degenerate two-level excitation to independent two-state systems," Phys. Rev. A **27**, 906–912 (1983).
[28]C. Godsil, "State transfer on graphs," Discrete Math. **312**(1), 129–147 (2012).
[29]M. Born and V. Fock, "Beweis des Adiabatensatzes," Z. Phys. **51**, 165–180 (1928).
[30]A. M. Childs, E. Farhi, and J. Preskill, "Robustness of adiabatic quantum computation," Phys. Rev. A **65**, 012322 (2001).
[31]K. Xu, R. Williams, S.-H. Hong, Q. Liu, and J. Zhang, "Semi-bipartite graph visualization for gene ontology networks," in *Graph Drawing*, Lecture Notes in Computer Science, edited by D. Eppstein and E. R. Gansner (Springer Berlin Heidelberg, 2010), pp. 244–255.
[32]O. M. Al-Kofahi and A. E. Kamal, "Network coding-based protection of many-to-one wireless flows," IEEE J. Sel. Areas Commun. **27**, 797–813 (2009).
[33]A. E. Brouwer and W. H. Haemers, *Spectra of Graphs*, Universitext (Springer-Verlag, New York, 2012).
[34]T. Hensgens, T. Fujita, L. Janssen, X. Li, C. J. Van Diepen, C. Reichl, W. Wegscheider, S. Das Sarma, and L. M. K. Vandersypen, "Quantum simulation of a Fermi–Hubbard model using a semiconductor quantum dot array," Nature **548**, 70–73 (2017).
[35]E. M. Graefe, H. J. Korsch, and D. Witthaut, "Mean-field dynamics of a Bose-Einstein condensate in a time-dependent triple-well trap: Nonlinear eigenstates, Landau-Zener models, and stimulated Raman adiabatic passage," Phys. Rev. A **73**, 013617 (2006).
[36]I. Bloch, J. Dalibard, and S. Nascimbène, "Quantum simulations with ultracold quantum gases," Nat. Phys. **8**, 267–276 (2012).
[37]L. M. K. Vandersypen, H. Bluhm, J. S. Clarke, A. S. Dzurak, R. Ishihara, A. Morello, D. J. Reilly, L. R. Schreiber, and M. Veldhorst, "Interfacing spin qubits in quantum dots and donors—Hot, dense, and coherent," npj Quantum Inf. **3**, 34 (2017).
[38]K. Groenland, "Adiabatic state distribution using anti-ferromagnetic spin systems," SciPost Phys. **6**, 011 (2019).
[39]A. D. Greentree, J. H. Cole, A. R. Hamilton, and L. C. L. Hollenberg, "Scaling of coherent tunneling adiabatic passage in solid-state coherent quantum systems," Proc. SPIE **5650**, 72–80 (2005).
[40]E. H. Lieb and D. W. Robinson, "The finite group velocity of quantum spin systems," Commun. Math. Phys. **28**, 251–257 (1972).
[41]M. Mitzenmacher and E. Upfal, *Probability and Computing* (Cambridge University Press, 2017).
[42]C. R. J. R. A. Horn, *Matrix Analysis* (Cambridge University Press, 1985).
[43]K. Groenland, "Quantum protocols for few-qubit devices," ILLC Dissertation Series (University of Amsterdam, 2020).